



Contents lists available at ScienceDirect

Thin Solid Films

journal homepage: [www.elsevier.com/locate/tsf](http://www.elsevier.com/locate/tsf)

# Influence of deposition conditions on the composition, texture and microstructure of RF-magnetron sputter-deposited hydroxyapatite thin films

A.A. Ivanova<sup>a</sup>, M.A. Surmeneva<sup>a</sup>, R.A. Surmenev<sup>a,c,\*</sup>, D. Depla<sup>b</sup>

<sup>a</sup> Department of Theoretical and Experimental Physics, Centre of Technology, National Research Tomsk Polytechnic University, 634050 Tomsk, Russia

<sup>b</sup> Research Group DRAFT, Department of Solid State Sciences, Ghent University, Krijgslaan 281/S1, 9000 Ghent, Belgium

<sup>c</sup> Fraunhofer Institute for Interfacial Engineering and Biotechnology IGB, 70569 Stuttgart, Germany

## ARTICLE INFO

Available online xxxx

### Keywords:

RF-magnetron sputtering  
Hydroxyapatite  
Substrate rotation  
Texture

## ABSTRACT

In this study, nanostructured hydroxyapatite (HA) coatings were deposited at a constant power via radio frequency magnetron sputtering. Substrate rotation was applied to increase the uniformity of the thin film properties. The crystallographic orientation, composition and microstructure of the coatings were examined. The characteristics of the deposited coatings associated with the applied deposition conditions were evaluated as a function of time that the samples spent under the target racetrack. The obtained thin films exhibit a change in out-of-plane orientation from preferential (002) to (300) and an increase in the Ca/P molar ratio when exposed for a longer time under the racetrack. This introduces the possibility of tuning crystallographic orientations of HA coatings.

© 2015 Elsevier B.V. All rights reserved.

## 1. Introduction

In the field of biomedical materials science, there are numerous studies devoted to the improvement of the biocompatibility and the osteoconductivity of implants. With this purpose, calcium phosphate (CaP) coatings have been deposited on the surface of different medical devices for decades. A typical example, which belongs to the family of widely used bone-substitute CaP materials, is hydroxyapatite (HA,  $\text{Ca}_{10}(\text{PO}_4)_6(\text{OH})_2$ ). HA's chemical similarity to the inorganic component of bones and teeth explains its high biocompatibility. A wide variety of techniques have been used to prepare CaP and, specifically, HA coatings. Some examples of these techniques are plasma spraying [1–3], magnetron sputter deposition [4–13], biomimetic crystallization techniques [14,15], electrophoretic deposition [16,17] and sol–gel synthesis [18, 19]. Radio frequency (RF) magnetron sputtering is an attractive method because it allows us to tune the coating properties and/or to modify the coating characteristics, such as the coating structure (amorphous or crystalline) and the Ca/P ratio [9]. However, this high flexibility makes RF-magnetron sputtering a rather complex method especially for the deposition of multicomponent materials, such as HA. Therefore, a detailed description of the processes occurring on the substrate surface and an in-depth characterization of the thin film properties are necessary because the morphological uniformity, phase purity and

crystallinity of the thin films are important parameters that strongly affect the biomedical application of HA modified surfaces. RF-magnetron sputtering is a line-of-sight deposition process where sputtered material is directed from a target towards a substrate. Therefore, substrate rotation is of crucial importance to coat complex substrates, such as medical implants. In the present study, continuous substrate rotation coupled with a rocking displacement of the centre of the substrate rotation axis was applied during RF-magnetron sputtering of the HA coating. This study has an objective to reveal the relationship between the deposition parameters and the film properties. This relationship will allow us to further develop strategies to obtain thin films with uniform and tailored properties.

## 2. Materials and methods

HA thin films were deposited via RF-magnetron sputtering. All of the depositions were performed in a vacuum chamber equipped with a RF-generator (13.56 MHz, COMDEL). The target had a diameter of 220 mm and a thickness of 9 mm. The target was prepared from a mechanochemically synthesized HA ( $\text{Ca}_{10}(\text{PO}_4)_6(\text{OH})_2$ ) precursor powder. The powder was uniaxially pressed at room temperature and subsequently sintered in air at 1100 °C for 1 h. The distance between the magnetron and the substrate holder was fixed at 40 mm. The substrate holder was rotated with a period of 85.7 s ( $T_c$ ). The latter movement was coupled with an arc displacement of the centre of the substrate holder with a rocking period of 600 s ( $T_{arc}$ ). The samples were mounted radially from the centre of the substrate holder. Prior

\* Corresponding author. Tel.: +7 903 953 09 69 (Tomsk), +49 157 802 268 04 (Stuttgart).

E-mail address: [rsurmenev@gmail.com](mailto:rsurmenev@gmail.com) (R.A. Surmenev).

to the depositions, the chamber was pumped down to a background pressure below  $8 \times 10^{-4}$  Pa using a turbo-molecular pump and a rotary pump. The pressure was adjusted to 0.4 Pa by introducing 90% Ar + 10% water (H<sub>2</sub>O) vapour into the chamber. The gas atmosphere and the ratio between Ar and the water vapour were controlled using conventional gas flow controllers. Pure, 1.5-mm-thick Ti (grade 2) plates and silicon were used as substrates ( $10 \times 10$  mm<sup>2</sup>). The titanium plates were chemically etched in an acid solution containing HF (48%) and HNO<sub>3</sub> (66%) dissolved in distilled water to a volume ratio of 1:2:2.5. After acid-etching, the samples were ultrasonically washed in ethanol followed by deionized water for 10 min at room temperature. The thickness of the deposited films was measured using ellipsometry (SE). The thickness and refractive index of the HA coatings deposited on the silicon substrates were determined by spectroscopic ellipsometry. The measurements were performed using the ELLIPS-1891 SAG setup (Russia) and the Woollam M-2000U equipment (Belgium). Chemical surface analysis was performed by X-ray photoelectron spectroscopy (XPS) using an S-Probe monochromatized XPS spectrometer (VG Scienta, UK) with an Al K $\alpha$  X-ray (1486.6 eV) monochromatic source. The take-off angle was 45° with a source voltage and power of 10 kV and 200 W, respectively. A base pressure of  $2 \times 10^{-9}$  mbar was obtained in the measuring chamber, and the analysis surface was 250  $\mu$ m  $\times$  1000  $\mu$ m. The sample surface was bombarded with 4 keV of Ar ions. To compensate for surface charging effects, an electron flood gun at 4 eV was employed. Survey scans (157.7 pass energy, 0.2 eV/step) were obtained in the 0–1300 eV range. Detailed scans (107.125 eV pass energy, 0.05 eV/step) were recorded for the O1s, C1s, Ca2p, and P2p regions. All of the XPS spectra were analysed using the Casa XPS software package (Version 2.3.16, Teignmouth, UK) taking into account the relative sensitivity factor of the different analysed elements [23]. The peak area for the most intense spectral line of each of the detected elemental species was used to determine the % atomic concentration. The effect of sample charging on the measured binding energy positions was corrected by setting the lowest binding energy component of the C1s spectral envelope to 284.6 eV, i.e., the value generally accepted for adventitious carbon surface contamination. Photoelectron spectra were processed by subtracting a linear background. The O1s, C1s, Ca2p, and P2p regions were decomposed using a Gaussian (70%)–Lorentzian (30%) product function to describe the peak shape and by imposing the number of components and the constraint that all components of a peak have the same FWHM. Peak assignments were carried out using values reported in the references given in the text. The difference in the 2p<sub>3/2</sub> and 2p<sub>1/2</sub> levels for the P2p peak and the Ca2p peak was 0.86 eV and 3.5 eV, respectively.

The microstructure of the films was assessed using a FEI Quanta 200 F scanning electron microscope applying a high voltage of 20 kV and a spot size of 3 arbitrary units. To reduce the surface charging effect, a thin Au film was deposited for 15 s before the analyses. The thin film texture was determined by X-ray diffraction (XRD, Bruker AXS) using Cu K $\alpha$  radiation in the Bragg–Brentano mode and a LynxEye Silicon Strip detector.

### 3. Results

#### 3.1. The deposition rate and the packing density

The refractive index and thin film thickness were evaluated using ellipsometry. The Cauchy dispersion model was used to fit the optical constants. The Fisher's correlation coefficient was applied to estimate the statistical significance of the obtained variables. Based on a statistical analysis, some outliers were excluded from further analysis, which resulted in a total of 29 studied samples. The deposition rate was calculated by dividing the measured thickness by the deposition time. The deposition rate versus the sample position related to the substrate holder centre is shown in Fig. 1.

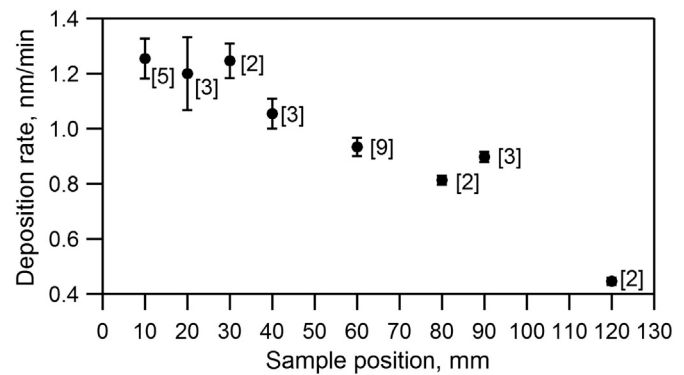


Fig. 1. Deposition rate as a function of the sample position from the substrate holder centre. The number of the analysed samples is given in brackets.

There was little variability in the data obtained from the samples positioned close to the edge of the substrate holder which is caused by the high uniformity of these layers compared with the coating deposited at the substrate holder centre. The film homogeneity is considered to be better at the edge of the moving substrate holder as the sample located there travels a longer distance and is less prone to a slight variation in the deposition process. Small deviations, despite the effort to minimize them, in the sample position will be more important for the samples in the centre of the substrate holder that could explain the dependency of the error as a function of the sample position on the substrate holder.

The packing density of the coatings was calculated using the following correlation [20,21]:

$$p = \frac{(n_f^2 - 1)(n_b^2 + 2)}{(n_f^2 + 2)(n_b^2 - 1)} \quad (1)$$

where  $n_f$  is the refractive index of the film, and  $n_b$  is the refractive index of the bulk materials. The  $n_f$  value at a wavelength of 638 nm was used in the calculations. A typical example of the dispersion curve is shown in Fig. 2a. Because there are no data available on the refractive index of the bulk HA at the applied laser wavelength, the refractive index of pure, bulk HA of 1.641 reported in the literature [22] was used as the reference ( $n_b$ ). The studied coatings revealed greater refractive index values and, hence, greater packing densities compared with the packing densities of the bulk HA (Fig. 2b). In this case, correlation (1) was used to estimate the difference in the packing density among the samples. Therefore, we concluded that the packing density of the majority of the sputter-deposited films was approximately 100% and did not depend on the sample position relative to the target erosion profile.

#### 3.2. Coating composition

The composition and chemical states of the coated samples were analysed via XPS. Curve-fitting demonstrated significant similarities in the chemical bonding for all of the films studied. Fig. 3 shows a typical XPS survey scan and the fitting results of the high-resolution regions. The O1s region obtained for these coatings exhibited two clear components, which occurred at 531.3 eV and 532.2 eV and indicates the presence of hydrogen phosphate groups [24,25]. The analysis of the Ca2p region indicated a well-resolved doublet that was located at approximately 347.6 and 351.1 eV, which correspond to the Ca2p<sup>3/2</sup> and Ca2p<sup>1/2</sup> components, respectively. The P2p region could be fitted with a doublet, which corresponds to P2p<sup>3/2</sup> and P2p<sup>1/2</sup> with a typical multiplet splitting. No clear trends could be found between the deposition conditions and the peak positions of O1s, P2p and Ca2p.

Nevertheless, the XPS analysis showed a clear trend between the Ca to P ratio as a function of the sample position (see Fig. 4).

Download English Version:

<https://daneshyari.com/en/article/10669640>

Download Persian Version:

<https://daneshyari.com/article/10669640>

[Daneshyari.com](https://daneshyari.com)